

The effect of local dipole moments on the structure and lattice dynamics of $\text{K}_{0.98}\text{Li}_{0.02}\text{TaO}_3$

Jinsheng Wen,^{1,2} Guangyong Xu,¹ C. Stock,^{3,4,*} P. M. Gehring,⁴ Z. Zhong,⁵ L.A. Boatner,⁶ E. L. Venturini,⁷ and G. A. Samara⁷

¹Condensed Matter Physics and Materials Science Department,
Brookhaven National Laboratory, Upton, New York 11973

²Department of Materials Science and Engineering, Stony Brook University, Stony Brook, New York 11794

³Physics Department, the Johns Hopkins University, Baltimore, Maryland, 21218

⁴NIST Center for Neutron Research, National Institute of Standards and Technology, Gaithersburg, Maryland 20899

⁵National Synchrotron Light Source, Brookhaven National Laboratory, Upton, New York 11973

⁶Oak Ridge National Laboratory, Oak Ridge, Tennessee 37831

⁷Sandia National Laboratories, Albuquerque, New Mexico 87185

(Dated: October 30, 2018)

We present high energy x-ray (67 keV) and neutron scattering measurements on a single crystal of $\text{K}_{1-x}\text{Li}_x\text{TaO}_3$ for which the Li content ($x = 0.02$) is less than $x_c = 0.022$, the critical value below which no structural phase transitions have been reported in zero field. While the crystal lattice does remain cubic down to $T = 10$ K under both zero-field and field-cooled ($E \leq 4$ kV/cm) conditions, the Bragg peak intensity changes significantly at $T_C = 63$ K. A strong and frequency-dependent dielectric permittivity, a defining characteristic of relaxors is observed at ambient pressure. However an extensive search for static polar nanoregions, which is also widely associated with relaxor materials, detected no evidence of elastic neutron diffuse scattering between 300 K and 10 K. Neutron inelastic scattering methods were used to characterize the transverse acoustic and optic phonons (TA and TO modes) near the (200) and (002) Bragg peaks. The zone center TO mode softens monotonically with cooling but never reaches zero energy in either zero field or in external electric fields of up to 4 kV/cm. These results are consistent with the behavior expected for a dipolar glass in which the local polar moments are frozen and exhibit no long-range order at low temperatures.

PACS numbers: 61.05.fg, 61.05.cf, 77.80.Dj, 77.84.Dy

I. INTRODUCTION

A defining feature of relaxor ferroelectrics is a large and highly frequency-dependent dielectric permittivity that exhibits a broad peak at a temperature that is not associated with a long-range ordered structural phase transition.¹ Among such materials the lead-oxide relaxors $(1-x)\text{Pb}(\text{Mg}_{1/3}\text{Nb}_{2/3})\text{O}_3$ - $x\text{PbTiO}_3$ (PMN- x PT)^{2,3,4} and $(1-x)\text{Pb}(\text{Zn}_{1/3}\text{Nb}_{2/3})\text{O}_3$ - $x\text{PbTiO}_3$ (PZN- x PT)^{5,6} have attracted the greatest attention because of the enormous potential they possess for use in device applications and because of the interesting scientific challenges they present to researchers attempting to understand the physics of systems in which order and disorder coexist and compete. Random fields arising from the heterovalent cations located on the perovskite B-sites are believed to be a seminal ingredient that underlies the properties of relaxors.⁷ At the same time, KTaO_3 , a perovskite compound that is known as an "incipient" ferroelectric because it does not undergo a ferroelectric transition in zero field⁸ even though the transverse optic (TO) phonon mode softens substantially at low temperature⁹, has long been of interest to scientists because the material properties can be changed dramatically by adding very small amounts of impurities. The Li-doped material $\text{K}_{1-x}\text{Li}_x\text{TaO}_3$, or $\text{KLT}(x)$, for example, transforms to a tetragonal phase for Li concentrations as low as $x_c = 0.022$ (below this critical value no structural phase transition has been observed). Surprisingly, $\text{KLT}(x)$, which contains no heterovalent cations and thus has comparatively little to no random fields, has also been reported to exhibit dielectric properties characteristic of relaxors for Li concentrations $x \geq x_c$.¹⁰

$\text{KLT}(x)$ has been extensively characterized using dielectric

spectroscopy, polarization hysteresis loops,^{10,11} Raman^{12,13,14}, and hyper-Raman scattering techniques¹⁵. As with other relaxor systems the concept of polar nanoregions (PNR) has been invoked to explain much of the experimental data on $\text{KLT}(x)$. These PNR are nanometer-scale regions of randomly-oriented, local polarization that first appear at high temperature within the paraelectric phase¹⁶ and give rise to strong, temperature-dependent diffuse scattering. However only a few studies have published data on the x-ray¹⁷ and neutron diffuse scattering¹⁸ observed in $\text{KLT}(x)$, which represent the most direct evidence of PNR. For $\text{KLT}(0.06)$ and $\text{KLT}(0.13)$ Yong *et al.*¹⁹ found strong diffuse scattering intensity around the (110) Bragg peak in the shape of rods extending along cubic $\langle 100 \rangle$ directions, but no diffuse intensity near (100) and (200). Wakimoto *et al.*²⁰ performed dielectric and neutron scattering measurements on $\text{KLT}(0.05)$ and also observed the formation of PNR upon cooling to low temperature. These studies suggest that the behavior of PNR in $\text{KLT}(x > 0.022)$ is similar to that reported in other relaxor systems such as PMN- x PT^{2,3,4} and PZN- x PT^{5,6}. But the situation for $\text{KLT}(x)$ at concentrations of Li below x_c remains unclear.

In this paper we focus on the properties of a $\text{KLT}(0.02)$ single crystal, for which the Li content lies just below the critical concentration. Dielectric measurements show that the temperature T_m , where the real part of the dielectric permittivity reaches a maximum, shifts from about 60 K to 90 K as the measurement frequency changes from 100 Hz to 1 MHz under a pressure of 1 bar (Fig. 1). This behavior is believed to result from a relaxation process involving local Li^+ dipole moments and $\text{Li}^+ - \text{Li}^+$ ion pairs. A key question is whether or not there are local regions around these dipoles that are polar

and form PNR. Both high-energy x-ray and neutron scattering techniques have been used to look for evidence of diffuse scattering that might indicate the presence of PNR in KLT(0.02). But in contrast to other relaxors and KLT(x) crystals with higher Li concentrations, no static diffuse scattering intensity is observed in this sample down to $T = 10$ K. This indicates that in KLT(x) for $x < x_c$, the local Li moments are mostly isolated and do not form larger (static) PNR.

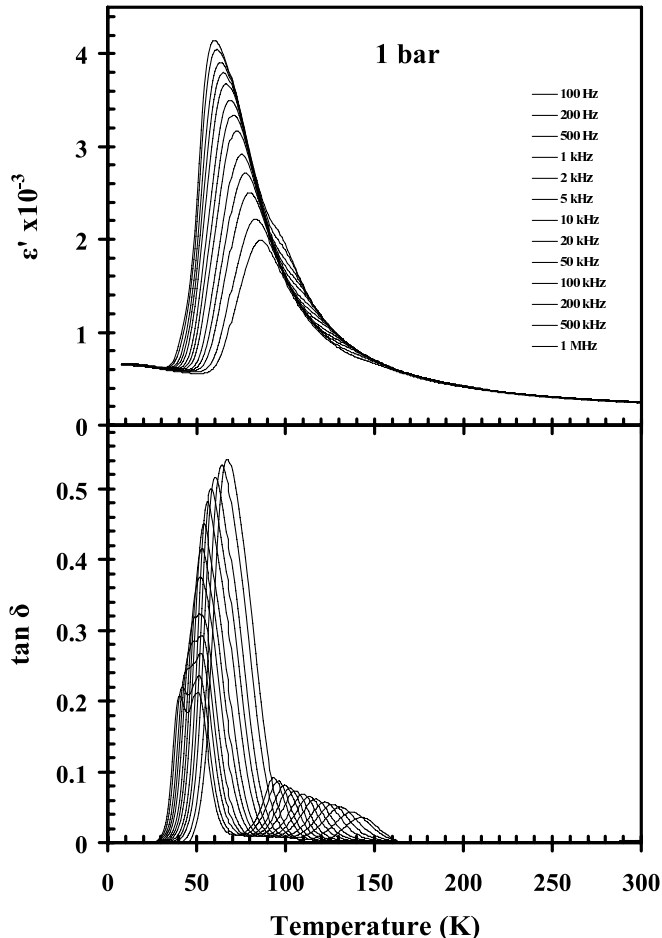


FIG. 1: Dielectric constant ϵ' and loss-tangent $\tan\delta$ of KLT(0.02) measured at different frequencies under a pressure of 1 bar.

Based on the shape of thermal diffuse scattering measured with high-energy x-rays, we have confirmed that the TO phonon polarized along $\langle 100 \rangle$ in this crystal is soft, which is consistent with the (expected) tetragonal polarization scheme in KLT compounds. In addition, no explicit structural changes in the crystal lattice structure are observed under both zero-field cooled (ZFC) and field-cooled (FC) conditions. However there is an increase in the Bragg peak intensity at $T_C = 63$ K, which suggests a possible lowering of crystal symmetry through a release of extinction. Low-energy acoustic and optic phonons were also studied with neutron inelastic scattering methods. The ZFC phonon behavior is very similar to that in the parent compound²¹ and in KLT(0.05)²⁰, where a softening, but no condensation and/or recovery, of the zone-center optic mode occurs. When cooled under an external electric field

$E = 4$ kV/cm oriented along the [001] direction, the crystal structure and energies of the TO/TA phonons are barely affected, whereas the intensities of long-wavelength phonons show interesting changes. Our results suggest that for small Li contents, KLT(x) changes from an incipient ferroelectric to a dipolar glass, where the dipole moments are frozen locally without long-range ferroelectric order.

II. EXPERIMENT

The KLT(0.02) single crystal examined in this study has dimensions $0.5 \text{ cm} \times 1 \text{ cm} \times 2 \text{ cm}$ and was grown at Oak Ridge National Laboratory. The crystal structure is cubic with a room temperature lattice constant $a = 3.992 \text{ \AA}$. The Li concentration of the crystal was estimated from the amount of Li in the melt and then corroborated from the established relationship between the Li concentration and the peak temperature of the dielectric permittivity, investigated by dielectric spectroscopy with measurements of the real (ϵ') and loss ($\tan\delta$) parts of the dielectric function.²² The set up for dielectric measurements is the same as that described in Ref. 20.

Neutron scattering experiments were carried out on the cold neutron triple-axis spectrometer SPINS and the thermal neutron triple-axis spectrometer BT7, which are located at the NIST Center for Neutron Research (NCNR). Horizontal neutron beam collimations of guide-80'-S-80'-open (S=sample) and 50'-50'-S-40'-240' were used for the measurements on SPINS and BT7, respectively. All data were taken in a fixed final energy mode (5.0 meV for SPINS and 14.7 meV for BT7) using the (002) Bragg reflection from highly-oriented pyrolytic graphite (HOPG) crystals to monochromate the incident and scattered neutrons. During the experiments on SPINS a Be filter was placed before and after the sample to reduce the scattering from higher order reflections; a single HOPG filter was placed after the sample on BT7 for the neutron inelastic measurements. All data were taken in the (HOL) scattering plane defined by the vectors [100] and [001], and described in terms of reciprocal lattice unit (rlu), where $1 \text{ rlu} = a^* = 2\pi/a = 1.574 \text{ \AA}^{-1}$. The electric field was applied along the [001] direction during the FC measurements. All data were taken on cooling from 300 K to ensure that all residual (poling) effects were removed.

X-ray scattering experiments were performed at beamlines X17B1 and X22A located at the National Synchrotron Light Source (NSLS). A 67 keV x-ray beam with an energy-resolution $\Delta E/E = 10^{-4}$ was produced at X17B1 using a sagittal-focusing double-crystal Si (311) monochromator with both crystals oriented in the asymmetric Laue mode.²³ Charge coupled device (CCD) detector were used to perform monochromatic Laue-style measurements. In this type of configuration scattering intensities on a large part of the surface of the Ewald sphere can be measured simultaneously. Data were taken in the (HK0) and (HKK) zones. Further details about the x-ray diffuse scattering experimental set up are discussed in the paper by Xu *et al.*⁶ Structural measurements were also performed on the X22A beamline using an incident x-ray energy of 10.7 keV and a perfect Si crystal analyzer.

III. RESULTS AND DISCUSSION

A. Structure

The structure of KLT(0.02) was examined using elastic neutron scattering and x-ray diffraction methods. As shown in Fig. 2, there is no discernable change in the position or longitudinal width of the (200) Bragg peak between 300 K and 10 K. There is also no obvious difference between Bragg peaks measured at (200) and (002). Based on the BT7 instrumental wave-vector resolution, which is $\Delta Q/Q \sim 5 \times 10^{-3}$ full width at half maximum (FWHM), we can set an upper limit of $\lesssim 0.1\%$ on the tetragonality $c/a - 1$. Within this limit KLT(0.02) does not undergo a tetragonal lattice distortion down to $T = 10$ K. This is confirmed using higher resolution $\Delta Q/Q \sim 3 \times 10^{-4}$ x-ray diffraction measurements, with absence of change in lattice constant at the entire temperature range. However, the ZFC (200) Bragg peak intensity jumps at $T_C = 63$ K, as shown in the inset of Fig. 2. The Bragg peak intensity change is observed repeatedly under cooling and heating. This effect is quite common in ferroelectric systems where a release of extinction occurs when the system transforms to a lower symmetry phase, and a crystal breaks up into many domains.⁷ In KLT(0.02), however, there is no explicit tetragonal phase. In this case the increase in the Bragg peak intensity at $T_C = 63$ K may be due to crystal imperfections, which can result either from subtle shifts in the atomic positions in an otherwise cubic lattice, or from local strain/stress induced at low temperature.

The same measurements were performed on the sample after it was cooled in an external electric field $E = 4$ kV/cm applied along [001]. Neither the width nor the intensity of the Bragg peaks were affected, and a same Bragg peak intensity increase occurs at 63 K. Thus the application of a moderate electric field along [001] has no discernable effect on the average static structure of this system.

B. Diffuse scattering

Fig. 3 shows CCD images taken at 10 K and 300 K in the (HK0) zone. In this plane the diffuse scattering extends along the [100] or [010] direction, or both. For example, near the $(\bar{2}00)$ Bragg peak the diffuse scattering is transverse in character in that it extends primarily along [010], whereas the diffuse scattering near $(\bar{2}10)$ extends along both [100] and [010]. These observations hold true at 10 K and 300 K and are qualitatively similar to those measured in other KLT(x) systems.^{19,20} However the diffuse intensities increase with temperature indicating that these measurements may be dominated by thermal diffuse scattering.

To obtain a complete picture of the diffuse scattering in three dimensions we rotated the sample about [100] by 45° and measured diffuse scattering intensities in the (HKK) zone. Fig. 4 shows the corresponding CCD images obtained at 10 K and 300 K. The sample was also tilted about the [011] direction by 2° to better observe the out-of-plane components of the diffuse scattering (for a detailed description of this tech-

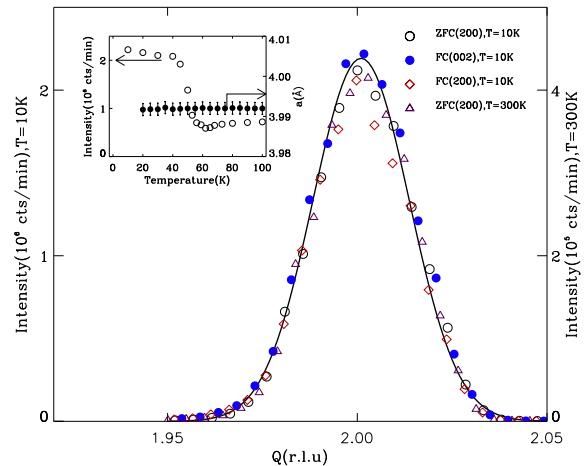


FIG. 2: (Color online) ZFC (200) Bragg peak scan at 300 K, ZFC and FC (200) and (002) Bragg peak scans at 10 K. The intensities of the 300 K data were scaled to permit a direct comparison with those at 10 K. The inset shows the ZFC (200) Bragg peak intensity measured with neutrons on BT-7 and the ZFC lattice parameters measured with x-rays on X22A. Uncertainties in the Bragg intensities are commensurate with the scatter in the data. The error bars in the inset are obtained by least-square fitting the data with Gaussian functions. The solid line is a guide for the eyes.

nique see Ref. 6). Near $(\bar{2}00)$ we observe diffuse scattering that extends along [011], whereas near $(\bar{1}11)$ the diffuse scattering extends along both [100] and [011]. Combining these data with those from the (HK0) zone, we find that the diffuse scattering in KLT(0.02) forms $\{001\}$ planes rather than rods oriented along $\langle 001 \rangle$. By contrast, the diffuse scattering measured in the lead-oxide relaxor PZN forms ellipsoids that are extended along $\langle 110 \rangle$.⁶ The planar geometry of the diffuse scattering in KLT(0.02) was confirmed after we tilted the sample so that the Ewald sphere was displaced even further from the Bragg peaks; then we could actually observe a splitting of the diffuse scattering intensities in the (010) and (001) plane, showing two almost vertical lines near (211) on the CCD image. Note that the diffuse scattering from all three planes ((100), (010), and (001)) is not always present around all Bragg peaks. For example, near (200) only the intensity from the (100) plane is observed while intensities in the (010) and (001) planes are absent. This is because the neutron (and x-ray) diffuse scattering cross section resulting from local atomic shifts is proportional to $|\mathbf{Q} \cdot \boldsymbol{\epsilon}|^2$, where $\boldsymbol{\epsilon}$ is the polarization vector. We can therefore carry out a simple polarization analysis similar to that done in Ref. 6. Our analysis shows that the diffuse scattering intensity from $\{001\}$ planes arises from polarizations oriented along $\langle 001 \rangle$, i. e. perpendicular to the planes. This indicates that the phonon mode polarized along $\langle 100 \rangle$ is soft, which is perfectly natural for a system that has a tetragonal ground state. By comparison, in the case of the lead-oxide relaxors (e. g. PMN- x PT and PZN- x PT) the phonon mode polarized along $\langle 110 \rangle$ is soft and the ground state is rhombohedral.^{6,24}

One disadvantage of x-ray diffuse scattering measurements

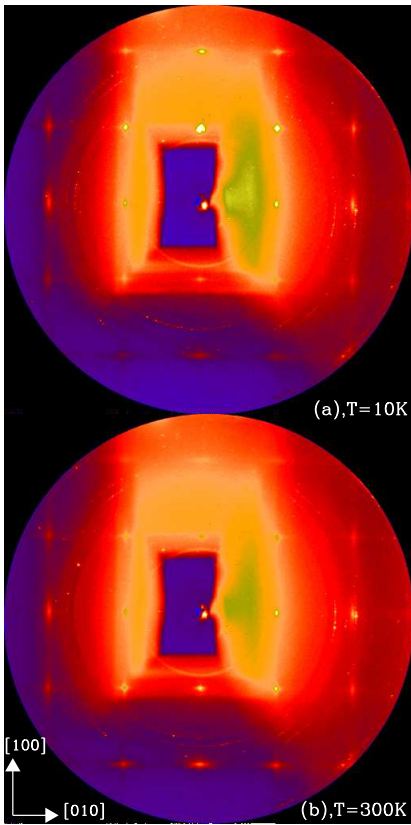


FIG. 3: (Color online) CCD images showing the diffuse scattering from KLT(0.02) measured at $T = 10$ K and 300 K in the (HK0) zone. The incident x-ray beam is oriented along [001].

is the lack of energy resolution; this makes it difficult to distinguish dynamic contributions, e. g. phonons or dynamic PNR, from static contributions. There have been some reports^{19,20} that the diffuse scattering in KLT(x) for $x > x_c$ is mainly static, as is the case in the lead-oxide relaxors PMN- x PT² and PZN- x PT⁶. However, in KLT(0.02) the x-ray diffuse scattering intensity increases with temperature, which is inconsistent with the behavior observed in these other relaxor systems where the diffuse scattering from static PNR decreases with temperature. Comès and Shirane reported that phonon contributions dominate the x-ray diffuse intensity in the parent compound KTaO_3 ²⁵, which strongly suggests that thermal diffuse scattering may dominate in KLT(x) samples with very low Li contents. In order to resolve this issue for KLT(0.02), we performed neutron scattering measurements using the NCNR SPINS spectrometer, which provided very good energy resolution (~ 0.34 meV FWHM).

Fig. 5 shows scans of the elastic scattering intensity as a function of the wavevector measured on SPINS along [100] and [010] at 10 K, 150 K and 300 K near the (100) and (110) Bragg peaks. The Bragg peaks were fit using resolution-limited Gaussian functions. The background is ~ 500 counts/2 min and is nearly temperature independent and identical at each Bragg peak. Diffuse scattering should be weak and broad compared to that from the Bragg peaks, appearing as broad tails on either side of the Bragg peak. How-

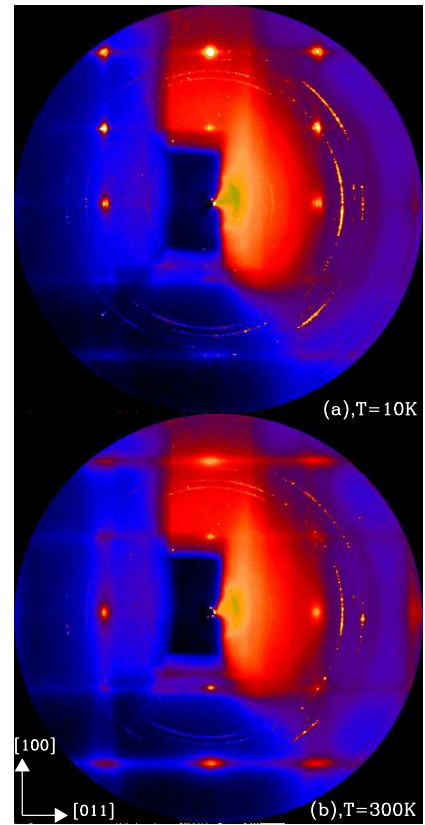


FIG. 4: (Color online) CCD images showing the diffuse scattering from KLT(0.02) measured at 10 K and 300 K in the (HKK) zone. The incident x-ray beam is oriented along [011].

ever, for KLT(0.02) we find that outside of both Bragg peaks the scattering intensity is flat and temperature independent, indicating the absence of any elastic diffuse scattering.

Here we only measured diffuse scattering near (100) and (110) peaks. Since it is highly unlikely that diffuse scattering structure factors are weak near both Bragg peaks, we believe that the static diffuse scattering is extremely weak in KLT(0.02). These results can be compared directly to those on PMN measured on the same instrument near these same two peaks.³ The diffuse scattering from KLT(0.02) is at least one to two orders of magnitude weaker. We thus conclude that the diffuse x-ray scattering shown in Fig. 3 and Fig. 4 is thermal diffuse in nature, i. e. dominated by phonons. This situation is quite different from that observed in other relaxor systems, as the diffuse scattering has been shown to be mainly elastic in PMN- x PT^{2,26}, PZN- x PT⁶, and even KLT(x) at higher Li concentrations^{19,20}. We also measured the elastic diffuse scattering under an external electric field oriented along [001]. Again in contrast to the behavior observed in both PMN- x PT and PZN- x PT, no change in the diffuse scattering was observed up to $E = 4$ kV/cm.

In KLT(x) it is known that local Li displacements lead to local dipole moments. Yet despite the absence of any measurable diffuse scattering in our sample, and thus by inference any static PNR, these local Li dipoles apparently still contribute to the relaxation process that leads to a strongly

frequency-dependent dielectric permittivity. The clear difference between KLT(0.02) and other relaxor compounds in which PNR are observed^{2,6,20,27,28,29} is that for KLT(0.02) the local moments are indeed really “local,” i. e. they do not polarize the surrounding regions to form PNR that exceed a few unit cells in size. Further, no correlations between local Li moments are evident from our measurements. With increasing Li concentration, the effect of these local polar moments on the bulk system becomes stronger, as evidenced by both the existence of static diffuse scattering (larger PNR) and an explicit phase transition into a low temperature tetragonal phase (for $x > x_c$). Whether these two effects are independent or correlated has yet to be determined.

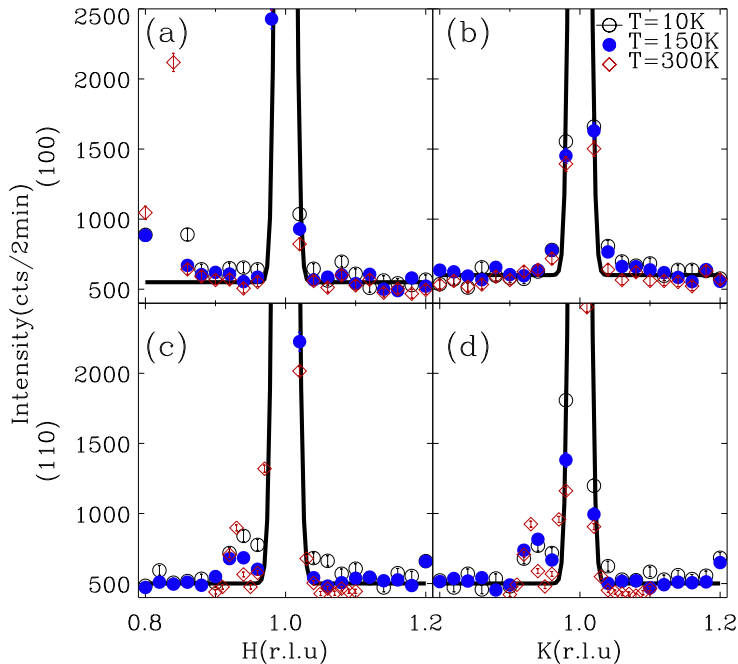


FIG. 5: (Color online) Elastic scans at 10 K, 150 K and 300 K. (a), (b), H and K scans at (100); (c), (d), H and K scans at (110). Error bars represent square root of the counts. Lines are guides for the eyes.

C. Phonons under electric field

The lowest-energy TO and transverse acoustic (TA) phonons have been characterized near (200) and (002) using the BT7 thermal neutron triple-axis spectrometer. In Fig. 6 we plot the dispersions for the TA and TO phonons measured near (200) along $[0\bar{1}0]$ at various temperatures under ZFC conditions. From 300 K to 10 K the zone-center TO phonon clearly softens, but it never reaches zero energy. This behavior is very similar to that seen in both the parent compound $\text{K}\alpha\text{TaO}_3$ ²¹ and in KLT(0.05)²⁰. In fact at 10 K the zone-center TO energy is more than 6 meV, which is higher than that (~ 3 meV) in the parent compound KTaO_3 .²¹ Raman measurements¹² on a KLT(x) crystal with a similar Li content are consistent with ours for this TO phonon mode. These results clarify that the

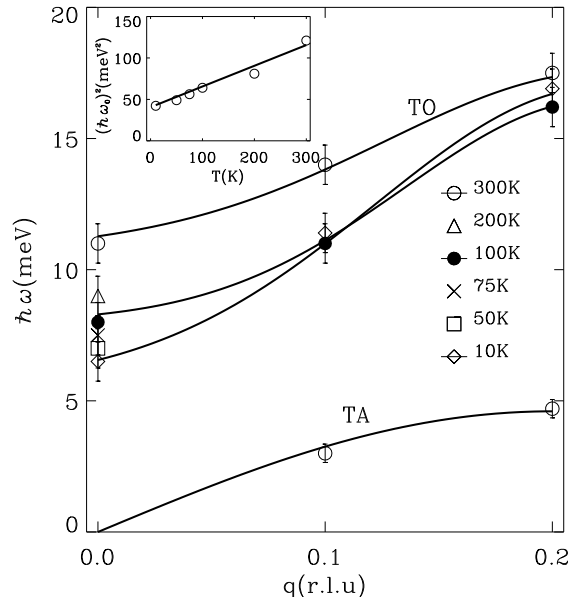


FIG. 6: Dispersion of TO and TA phonons under zero field at different temperatures. Measurements were taken near (200) along $[0\bar{1}0]$. The inset is a plot of $(\hbar\omega_0)^2$ vs. temperature. Error bars are obtained by least-square fitting the data with Lorentzian functions. Lines are guides for the eyes.

x-ray diffuse scattering intensity discussed previously arises from the TA phonon because the TA phonon lies lower in energy than the TO phonon, which never drops below 6 meV.

If we plot the soft mode energy $(\hbar\omega_0)^2$ v.s. temperature (see the inset to Fig. 6) we see that $(\hbar\omega_0)^2$ decreases linearly with T as expected for a conventional displacive ferroelectric. This behavior is also observed in the lead-oxide relaxors such as PMN at high temperature. However, unlike the case of PMN, the soft mode in KLT(0.02) never recovers as the linear decrease in $(\hbar\omega_0)^2$ persists down to at least 10 K. This is consistent with the absence of a ferroelectric phase transition for $T > 0$ and suggests that the local, polar moments freeze on cooling, which implies the presence of a low-temperature dipolar glass phase. At the same time, the energy width of the soft mode remains almost constant, yet larger than the instrument resolution, thus indicating a short phonon lifetime. This is similar to what is observed in KLT(0.05).²⁰ It is thus possible that the local dipole moments resulting from the large Li ionic displacements do interact with, or scatter, the soft mode, even though there is no clear temperature scale associated with this interaction. In this respect the soft mode in KLT(0.02) behaves quite differently from those measured in PMN- x PT, and PZN- x PT, where the so-called “waterfall” effect (i. e. a wavevector-dependent broadening of the soft mode in energy) is observed^{30,31,32} and lately interpreted in terms of a defect model arising from chemical and valence disorder³³. In our KLT(0.02) sample the Li content is relatively low; thus effects from chemical disorder are minimal and no “waterfall” effect is present.

Interestingly, the TA mode in KLT(0.02) behaves quite differently from that in KLT(0.05).²⁰ Unlike the more highly Li-doped samples, the TA phonon in our sample remains well-defined over the temperature range (10 K to 300 K). There is virtually no temperature dependent change in either the dispersion, lineshape, or linewidth of the TA mode. This suggests that the broadening of the TA mode reported in KLT(0.05) on cooling is very likely due to an interaction between the TA mode and the polar, short-range order (PNR). It seems plausible that as the PNR in KLT(0.05) grow larger on cooling, their interaction with the TA mode becomes stronger, causing a change of the TA phonon line width (lifetime). In KLT(0.02), since there is no static diffuse scattering, but only isolated local Li moments, the TA phonon mode remains unchanged.

When an electric field is applied along the [001] direction, we observe interesting changes in the phonon behavior. As shown by our structural measurements, no long-range, ferroelectric, tetragonal phase is induced when cooling under a moderate field. The phonon behavior is completely consistent with our structural results. At 10 K, the energy of the TA mode is unaffected by the external field, and any effect on the energies of the TO mode is very small (see the inset to Fig. 7). In other words, the FC energies of the TA and TO phonons remain close to the ZFC values in our sample in which there is no explicit low-temperature tetragonal phase. This finding stands in stark contrast to those measured in more highly doped KLT(x) samples, e. g. in KLT(0.035)¹⁸ where a clear splitting of the TA mode is observed when the system is cooled under a [001] field and transforms into a tetragonal phase. Ostensibly this is because the local dipole moments in KLT(0.02) are frozen, thus making it very difficult to drive the system into a long-range-ordered ferroelectric phase with an external field.

Despite the absence of a measurable change in phonon energies under an external field there is a significant change in the intensities and/or lineshapes of the TA/TO phonons measured near the (200) and (002) Bragg peaks. The intensity for the zone center TO mode measured near (200) increases and the peak becomes sharper, while near (002) the intensity of the TO mode decreases, and the peak becomes broader in energy. The difference between the intensities is as large as 50%. As q increases the effect appears to diminish. When $q = 0.1$ rlu, the difference in the optic modes measured near (200) and (002) is already tiny. At a wavevector of $q = 0.2$ rlu, the TA and TO phonons measured near (200) and (002) are very similar. We are puzzled, however, to note that the FC acoustic mode intensity near (002) increases significantly.

These changes suggest that even though no clear evidence of any long-range polar order is induced with the application of a moderate electric field oriented along [001], a field can still influence the overall polar structure of the system to a certain extent. It is likely that an electric field can lead to an enhancement of the local Li dipole moments polarized along [001]. This will lead to a stronger interaction between these local dipole moments and TO phonons having the same polarization ([001]). The result is the broadening of the zone center TO mode measured near (002). The change in the TA phonon mode indicates a strong coupling between TA and TO modes

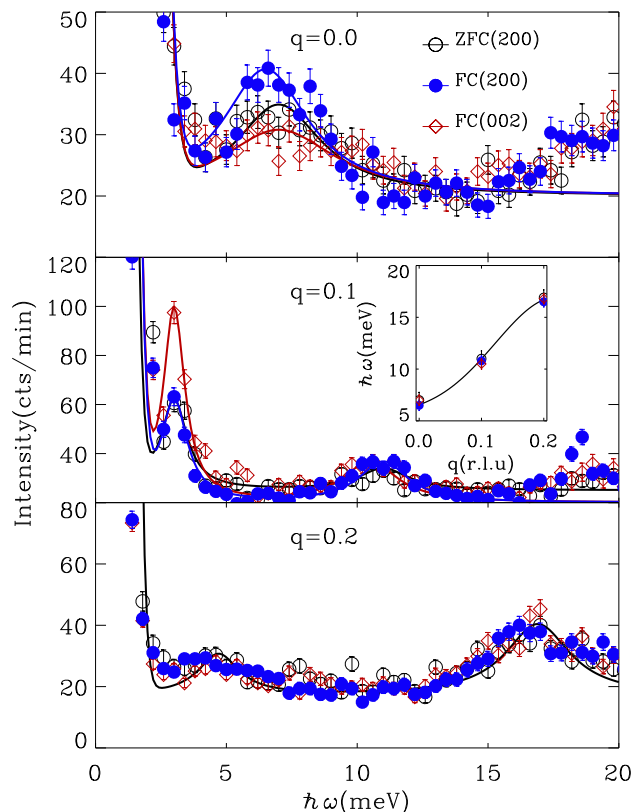


FIG. 7: (Color online) Constant q scans for $q = 0.0, 0.1, 0.2$ rlu, measured at 10 K. The inset shows TO phonon dispersion measurements under ZFC (open circles), FC(200) (closed circles), and FC(002) (diamonds) conditions. Intensity errors represent the square root of the counts, and error bars in the inset are obtained by least-square fitting the data with Lorentzian functions. Lines are guides for the eyes.

in the system, similar to that in its parent system KTaO_3 ²⁵, which should only be significant for small (but non-zero) q .

IV. SUMMARY

The strong frequency-dependent peak in the dielectric curve $\epsilon'(\omega, T)$ observed in KLT(0.02) would appear to justify categorizing it with other relaxor systems. Yet unlike other relaxors where static PNR are easily identified by the presence of strong, temperature dependent diffuse scattering, no such scattering is observed near either the (100) and (110) Bragg peaks between 10 K and 300 K. The diffuse planar diffuse scattering intensities observed with x-rays are dominated by contributions from soft phonon modes. This makes the system very unique. In KLT(0.02) the PNR are either small in volume (i. e. isolated local Li dipole moments) or dynamic in nature. In fact, these local Li dipole moments dominate the physics in this system.

Our structural measurements show no splitting of the main (200) Bragg peak in either ZFC or FC conditions. This suggests that the shape of the unit cell in KLT(0.02) remains cubic

down to low temperatures within the precision of our measurements ($\lesssim 0.1\%$). The change in Bragg peak intensity at $T_C = 63\text{ K}$ suggests that subtle changes in the crystal do occur at T_C . On the other hand, although the zone center energy of the TO phonon softens significantly with cooling, it does not condense at low temperature. No ferroelectric phase transition takes place under ZFC or FC conditions (for field strength up to 4 kV/cm), which is suggestive of a dipole glass phase in which the local moments are frozen and long-range polar order is not achieved.

Interesting electric field effects have been observed in our neutron measurements of the TO and TA modes for small $q < 0.20\text{ rlu}$. Although electric fields of up to 4 kV/cm oriented along $[001]$ fail to induce long-range polar order, the same fields appear to be able to affect the Li moments such that long wavelength TO phonons polarized along $[001]$ are more strongly scattered by the local Li moments, thus causing them to become broader in energy (shorter lifetimes). However, the system remains in a dipolar glass state where the

local Li moments are frozen and no long-range correlation between these moments exists, as also evidenced by the absence of static diffuse scattering under an external field.

Acknowledgments

We would like to thank stimulating discussions with H. J. Kang, J. H. Chung, J. W. Lynn, and Y. Chen. The work at Brookhaven National Laboratory was supported by the U. S. Department of Energy (DOE) under contract No. DE-AC02-98CH10886. C. Stock was supported by Natural Sciences and Engineering Research Council of Canada and the NSF under Grants No. DMR-0306940. Research at ORNL is sponsored by the Division of Materials Sciences and Engineering, Office of Basic Energy Sciences, U. S. DOE, under contract DE-AC05-00OR22725 with Oak Ridge National Laboratory, managed and operated by UT-Battelle, LLC.

-
- * Also at ISIS, Rutherford Appleton Laboratory, UK.
- ¹ G. Smolensky and A. I. Agranovskaya, *Sov. Phys. Solid State* **1**, 1429 (1960).
 - ² Guangyong Xu, G. Shirane, J. R. D. Copley, and P. M. Gehring, *Phys. Rev. B* **69**, 064112 (2004).
 - ³ H. Hiraka, S.-H. Lee, P. M. Gehring, G. Xu, and G. Shirane, *Phys. Rev. B* **70**, 184105 (2004).
 - ⁴ S. N. Gvasaliya, S. G. Lushnikov, and B. Roessli, *Phys. Rev. B* **69**, 092105 (2004).
 - ⁵ J. Hlinka, S. Kamba, J. Petzelt, J. Kulda, C. A. Randall, and S. J. Zhang, *J. Phys.: Condens. Matter* **15**, 4249 (2003).
 - ⁶ Guangyong Xu, Z. Zhong, H. Hiraka, and G. Shirane, *Phys. Rev. B* **70**, 174109 (2004).
 - ⁷ C. Stock, R. J. Birgeneau, S. Wakimoto, J. S. Gardner, W. Chen, Z.-G. Ye, and G. Shirane, *Phys. Rev. B* **69**, 094104 (2004).
 - ⁸ S. H. Wemple, *Phys. Rev.* **137**, A1575 (1965).
 - ⁹ J. D. Axe, J. Harada, and G. Shirane, *Phys. Rev. B* **1**, 1227 (1970).
 - ¹⁰ J. Toulouse, B. Vugmeister, and R. Pattnaik, *Phys. Rev. Lett.* **73**, 3467 (1994).
 - ¹¹ J. Toulouse, P. DiAntonio, B. E. Vugmeister, X. M. Wang, and L. A. Knauss, *Phys. Rev. Lett.* **68**, 232 (1992).
 - ¹² P. Calvi, P. Camagni, E. Giulotto, and L. Rollandi, *Phys. Rev. B* **53**, 5240 (1996).
 - ¹³ R. Prater, L. Chase, and L. Boatner, *Phys. Rev. B* **23**, 5904 (1981).
 - ¹⁴ P. DiAntonio, B. E. Vugmeister, J. Toulouse, and L. A. Boatner, *Phys. Rev. B* **47**, 5629 (1993).
 - ¹⁵ H. Vogt, *J. Phys.: Condens. Matter* **7**, 5913 (1995).
 - ¹⁶ G. Burns and F. H. Dacol, *Phys. Rev. B* **28**, 2527 (1983).
 - ¹⁷ S. Andrews, *J. Chem. Phys.* **18**, 239 (1985).
 - ¹⁸ J. Toulouse and B. Hennion, *Phys. Rev. B* **49**, 1503 (1993).
 - ¹⁹ G. Yong, J. Toulouse, R. Erwin, S. M. Shapiro, and B. Hennion, *Phys. Rev. B* **62**, 14736 (2000).
 - ²⁰ S. Wakimoto, G. Samara, R. Grubbs, E. Venturini, L. Boatner, G. Xu, G. Shirane, and S.-H. Lee, *Phys. Rev. B* **74**, 054101 (2006).
 - ²¹ E. Farhi, A. Tagantsev, R. Currat, B. Hehlen, E. Courtens, and L. Boatner, *Eur. Phys. J. B* **15**, 615 (2000).
 - ²² G. Samara, *Solid State Physics* **56**, 239 (2001).
 - ²³ Z. Zhong, C. C. Kao, D. P. Siddons, and J. B. Hastings, *J. Appl. Cryst.* **34**, 646 (2001).
 - ²⁴ C. Stock, H. Luo, D. Viehland, J.-F. Li, I. Swainson, R. J. Birgeneau, and G. Shirane, *J. Phys. Soc. Japan* **74**(11), 3002 (2005).
 - ²⁵ R. Comès and G. Shirane, *Phys. Rev. B* **5**, 1886 (1972).
 - ²⁶ M. Matsuura, K. Hirota, P. M. Gehring, Z.-G. Ye, W. Chen, and G. Shirane, *Phys. Rev. B* **74**, 144107 (2006).
 - ²⁷ A. Naberezhnov, S. Vakhruhev, B. Doner, D. Strauch, and H. Moudden, *Eur. Phys. J. B* **11**, 13 (1999).
 - ²⁸ S. B. Vakhruhev, B. E. Kvyatkovskiy, A. A. Naberezhnov, N. M. Okuneva, and B. Toperverg, *Ferroelectrics* **90**, 173 (1989).
 - ²⁹ K. Hirota, Z.-G. Ye, S. Wakimoto, P. M. Gehring, and G. Shirane, *Phys. Rev. B* **65**, 104105 (2002).
 - ³⁰ P. M. Gehring, S. Wakimoto, Z.-G. Ye, and G. Shirane, *Phys. Rev. Lett.* **87**, 277601 (2001).
 - ³¹ P. M. Gehring, S.-E. Park, and G. Shirane, *Phys. Rev. Lett.* **84**, 5216 (2000).
 - ³² P. M. Gehring, S.-E. Park, and G. Shirane, *Phys. Rev. B* **63**, 224109 (2001).
 - ³³ C. Stock, D. Ellis, I. P. Swainson, Guangyong Xu, H. Hiraka, Z. Zhong, H. Luo, X. Zhao, D. Viehland, R. J. Birgeneau, and G. Shirane, *Phys. Rev. B* **73**, 064107 (2006).